1521-009X/48/10/1044–1052$35.00
Drug Metabolism and Disposition

https://doi.org/10.1124/dmd.120.000048
Drug Metab Dispos 48:1044–1052, October 2020

Special Section on Natural Products: Experimental Approaches to Elucidate Disposition Mechanisms and Predict Pharmacokinetic Drug Interactions

Influence of Zuojin Pill on the Metabolism of Venlafaxine in Vitro and in Rats and Associated Herb-Drug Interaction

Yue Li, Juan Li, Dongmin Yan, Qian Wang, Jingyi Jin, Bo Tan, and Furong Qiu

Laboratory of Clinical Pharmacokinetics, Shuguang Hospital Affiliated to Shanghai University of Traditional Chinese Medicine, Shanghai, China (Y.L., J.L., D.Y., Q.W., J.J., B.T., F.Q.) and Department of Pharmacy, Pudong New Area People's Hospital, Shanghai, China (J.L.)

Received March 26, 2020; accepted June 11, 2020

ABSTRACT

Venlafaxine (VEN), a first-line antidepressant, and Zuojin Pill (ZJP), a common Chinese herbal medicine consisting of *Rhizoma Coptidis* and *Fructus Evodiae*, have a high likelihood of combination usage in patients with depression with gastrointestinal complications. ZJP exhibits inhibitory effects on recombinant human cytochrome P450 isoenzymes (rhP450s), especially on CYP2D6, whereas VEN undergoes extensive metabolism by CYP2D6. From this perspective, we investigated the influence of ZJP on the metabolism of VEN in vitro and in rats for the first time. In this study, ZJP significantly inhibited the metabolism of VEN in both rat liver microsomes (RLM) and human liver microsomes (HLM); meanwhile, it inhibited the *O*-demethylation catalytic activity of RLM, HLM, rhCYP2D6*1/*1, and rhCYP2D6*10/*10, primarily through CYP2D6, with IC_{50} values of 129.9, 30.5, 15.4, and 2.3 μg/ml, respectively. Furthermore, the inhibitory effects of ZJP on hepatic metabolism and pharmacokinetics of VEN could also be observed in the pharmacokinetic study of rats. The area under drug concentration-time curve$_{0-24\ hour}$ of VEN and its major metabolite *O*-desmethylvenlafaxine (ODV) increased by 39.6% and 22.8%, respectively. The hepatic exposure of ODV decreased by 57.2% 2 hours after administration ($P = 0.014$). In conclusion, ZJP displayed inhibitory effects on hepatic metabolism and pharmacokinetics of VEN in vitro and in rats mainly through inhibition of CYP2D6 activity. The human pharmacokinetic interaction between ZJP and VEN and its associated clinical significance needed to be seriously considered.

SIGNIFICANCE STATEMENT

Zuojin Pill, a commonly used Chinese herbal medicine, demonstrates significant inhibitory effects on hepatic metabolism and pharmacokinetics of venlafaxine in vitro and in rats mainly through suppression of CYP2D6 activity. The human pharmacokinetic interaction between Zuojin Pill and venlafaxine and its associated clinical significance needs to be seriously considered.

Introduction

Venlafaxine (VEN), a selective serotonin and noradrenaline reuptake inhibitor, is one of the most efficacious and commonly prescribed antidepressants (Cipriani et al., 2018). VEN undergoes extensive metabolism by cytochrome P450 (CYP450) isoenzymes. Its major metabolite *O*-desmethylvenlafaxine (ODV) is predominantly catalyzed by CYP2D6, which has similar efficacy as VEN, whereas minor metabolites with little pharmacological effect, including *N*-desmethylvenlafaxine (NDV) and *N, O*-didesmethylvenlafaxine (NODV), are catalyzed by CYP2C9, CYP2C19, and CYP3A4 (Fig. 1) (Otton et al., 1996; Fogelman et al., 1999). The blood (including plasma) concentrations of VEN + ODV (active moiety) are considered clinically relevant to a relatively narrow therapeutic reference range (100–400 ng/ml) (Hiemke et al., 2018). The factors that may influence the pharmacokinetics of VEN, such as age, disease state, genetic polymorphism of metabolic enzymes, and drug combination, should also be considered seriously (Magalhães et al., 2015). Recently, increasing evidence has suggested that concomitant administration of CYP2D6 inhibitors may incur pharmacokinetic drug-drug interaction (DDI) of VEN (Jiang et al., 2015; Magalhães et al., 2015).

Zuojin Pill (ZJP) is a traditional Chinese herbal formula recorded in the Chinese Pharmacopoeia for treating gastrointestinal disorders (Chinese Pharmacopoeia Commission, 2015). It consists of two commonly used herbs, *Rhizoma Coptidis* and *Fructus Evodiae*, following a 6:1 (w/w) ratio. The primary active ingredients in ZJP are supposed to be alkaloid compounds such as *Rhizoma Coptidis* alkaloids berberine and coptisine and *Evodiae* alkaloids evodiamine and rutaecarpine (Gao et al., 2010; Wang et al., 2013). In previous studies, ZJP

This work was supported by the Shanghai Municipal Health Committee [Grant 201740199] and the Shanghai Shuguang Hospital [Grant SGXZ-201907].
https://doi.org/10.1124/dmd.120.000048.
This article has supplemental material available at dmd.aspetjournals.org.

ABBREVIATIONS: AUC, area under drug concentration-time curve; CL_{int}, intrinsic clearance; DDI, drug-drug interaction; HLM, human liver microsomes; K_m, Michaelis-Menten constant; KTZ, ketoconazole; LC-MS/MS, liquid chromatography–tandem mass spectrometry; NDV, *N*-desmethylvenlafaxine; NODV, *N, O*-didesmethylvenlafaxine; ODV, *O*-desmethylvenlafaxine; QND, quinidine; QNN, quinine; rhP450, recombinant human cytochrome P450 isoenzyme; RLM, rat liver microsomes; TCM, traditional Chinese medicine; VEN, venlafaxine; ZJP, Zuojin pill.

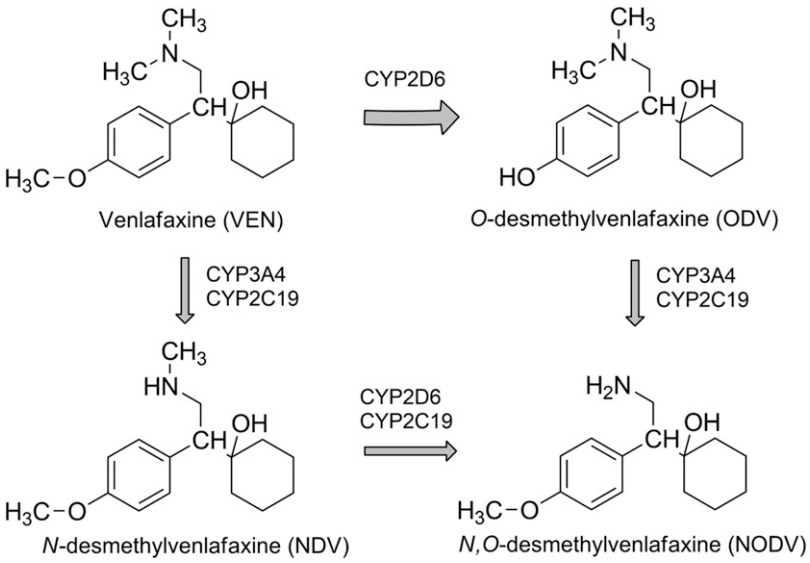

Fig. 1. The primary metabolic pathway of VEN in humans.

and its bioactive components, such as berberine and coptisine, exhibited inhibitory effects on CYP2D6, CYP1A2, and CYP3A4 in vitro (Han et al., 2011; Liu et al., 2014). Moreover, when ZJP is coadministered with dextromethorphan, a specific CYP2D6 prober substrate, the area under drug concentration-time curve $(AUC)_{0–24\ hour}$ of dextromethorphan in healthy CYP2D6*1/*1 carriers increases 3.0-fold (Qiu et al., 2016). Because of the concomitant symptoms of depression itself and the adverse reactions of antidepressants, patients with depression are usually accompanied by several gastrointestinal disorders, and there exists a high likelihood of the combination usage of ZJP and VEN in patients with depression with gastrointestinal complications (Qiu et al., 2015; Wang et al., 2020).

Herbs and natural products (including botanical dietary supplements and foods) can produce clinically significant pharmacokinetic interactions with conventional drugs (Johnson et al., 2018). Abnormally increased or decreased drug exposure caused by herbs and natural products will generate potential risks in clinical treatment. In the classic cases, St. John's wort and grapefruit juice can significantly influence the pharmacokinetics of cyclosporine and felodipine, respectively, which will further interfere with the therapeutic efficacy of both drugs (Paine and Oberlies, 2007; Nicolussi et al., 2020).

Therefore, in the present study, we investigated the influence of ZJP on the metabolism of VEN in human liver microsomes (HLM), rat liver microsomes (RLM), and recombinant human P450 enzymes (rhP450s). Moreover, the potential pharmacokinetic interaction between ZJP and VEN was evaluated by assessing the effects of ZJP on VEN and its metabolites in rats.

Materials and Methods

Chemicals and Materials. Venlafaxine hydrochloride (purity >99%) and ODV (purity >99%) were obtained from Selleck Chemicals (Houston, TX). NDV (purity >98%) and NODV (purity >98%) were purchased from Toronto Research Chemicals (Toronto, Canada). Berberine hydrochloride (purity ≥95%), coptisine hydrochloride (purity ≥98%), evodiamine (purity ≥99%), and rutaecarpine (purity ≥98%) were obtained from Aladdin (Shanghai, China). The pooled liver microsomes of rats (a total of 75 rats of the same sex) and humans (a total of 25 adult donors of the same sex) were obtained from the Research Institute for Liver Diseases Co., Ltd. (Shanghai, China) and BioIVT (Westbury, NY), respectively. Recombinant human CYP2D6*1 and CYP2D6*10 expressed in *Escherichia coli* were obtained from Cypex Ltd. (Scotland, UK). Reduced NADPH was obtained from Solarbio (Beijing, China). Diphenhydramine was purchased from Sigma-Aldrich (St. Louis, MO). All other reagents were of the highest quality commercially available.

Zuojin Pill (ZJP, batch number: 20180304) was purchased from Hubei Xianglian pharmaceutical Co., Ltd (Wuhan, Hubei, China). The ZJP dosing solutions were prepared as follows: briefly, Zuojin Pill was ground into powder and dissolved in DMSO for in vitro study, whereas for in vivo study, 10-fold volumes of deionized water were subsequently added. The method for determining the concentration of major alkaloid components in ZJP solution was similar to the liquid chromatography–tandem mass spectrometry (LC-MS/MS) method in a biologic matrix described below. The amounts of four major alkaloids in ZJP, namely berberine, coptisine, evodiamine, and rutaecarpine, were calculated as 25.5, 3.1, 0.31, and 0.48 mg/g, respectively (Supplemental Table 1).

Animals. Wistar rats (male, 180–220 g) were purchased from Charles River laboratory animal Co., Ltd. (Beijing, China). Rats were housed in a room at 16–26°C, with a light/dark cycle of 12/12 hours and humidity of 40%–70%. All animal experiments were approved by the Animal Care and Use Committee of Shanghai University of Traditional Chinese Medicine and followed the Guidance for the Care and Use of Laboratory Animals in China.

Metabolic Stability Assessment of VEN in HLM and RLM. The total volume of the incubation mixture was 200 μl, which included VEN (1 μM), HLM (1.0 mg/ml) or RLM (0.5 mg/ml), and NADPH (10 mM), in 100 mM potassium phosphate-buffered solution (PBS) (pH 7.4). The reaction was conducted in a shaking water bath at 37°C for 60 minutes. To quench the reaction, 200 μl of ice-cold methanol containing diphenhydramine (100 ng/ml) as an internal standard was added. The mixture was vortexed for 1 minute and centrifuged at 15,000*g* at 4°C for 5 minutes. Finally, the supernatant was collected and injected into a high-performance LC-MS/MS analysis. The VEN depletion data were used for calculating enzymatic parameters.

Enzymatic Kinetics Assessment of VEN in RLM, HLM, and rhP450s. Preliminary experiments were conducted to determine the optimal conditions for linear product formation, such as protein concentration and incubation time with RLM, HLM, and rhCYPs, respectively. Subsequent experiments were conducted under the conditions of linear product formation. For both HLM and RLM experiments, the reaction mixture containing 0.2 mg/ml of microsomes and VEN (0.2–750 μM) in 100 mM PBS buffer (pH 7.4) was preincubated at 37°C for 5 minutes. Then, the mixture was incubated with 10 mM NADPH at 37°C for 15 minutes. For rhCYP2D6*1*1 or *10*10, the reaction mixture containing 8 pmol/ml of each enzyme and VEN (0.04–150 μM for CYP2D6*1*1 and 2–1500 μM for CYP2D6*10*10) was preincubated at 37°C for 5 minutes, followed by another 15-minute incubation after the addition of 10 mM NADPH. As described above, all reactions were quenched and treated with ice-cold methanol, and the supernatant was collected for LC-MS/MS analysis. The ODV formation data were used for calculating enzymatic parameters.

Evaluation of the Influences of ZJP and Its Major Components on the Metabolism of VEN In Vitro. The influences of ZJP and its major components,

TABLE 1

Mass spectrometry parameters for measuring VEN and its metabolites, ODV, NDV, and NODV

Analytes	Transition (*m/z*)	Spray Voltage (V)	Temp. (°C)	DP (V)	CE (V)	CXP (V)	EP (V)
VEN	278.2 > 58.1	5500	400	46	46	12	10
ODV	264.2 > 58.1	5500	400	46	46	12	10
NDV	264.2 > 246.1	5500	400	35	14	12	10
NODV	250.2 > 232.1	5500	400	30	14	12	10
Diphenhydramine	256.0 > 167.1	5500	400	46	25	12	10

Temp., temperature. DP, declustering potential. CE, collision energy. CXP, CXP, cell exit potential. EP, entrance potential.

berberine and coptisine, on the metabolism of VEN were conducted with RLM and HLM, respectively. HLM (1.0 mg/ml) or RLM (0.5 mg/ml) were preincubated with VEN (1 μM), ZJP (150 μg/ml), berberine, or coptisine (30 μM) at 37°C for 5 minutes. Control samples were prepared in the absence of the following inhibitors: quinidine (QND, a human CYP2D6 inhibitor, 2 μM), quinine (QNN, a rat CYP2D inhibitor, 2 μM), and ketoconazole (KTZ, a CYP3A4 inhibitor, 2 μM). All reactions were initiated with 10 mM NADPH, lasted for 15 minutes at 37°C, and were terminated with 200 μl of ice-cold methanol containing 100 ng/ml diphenhydramine.

To determine the half-maximal inhibitory concentration (IC_{50}) of ZJP and its major components coptisine and berberine toward the metabolism of VEN, a series of concentrations of the above drugs were preincubated with RLM, HLM, and rhCYP2D6s, respectively. For microsomes studies, HLM (1 mg/ml) or RLM (0.5 mg/ml) were preincubated with VEN (0.02 μM for HLM and 1 μM for RLM), ZJP (0.71–287.56 μg/ml for HLMs and 0.142–575.12 μg/ml for RLMs), or its major components coptisine (0.1–100 μM for HLM and 0.1–200 μM for RLM) and berberine (1–500 μM for HLMs and 1–1000 μM for RLMs) at 37°C for 5 minutes. For rhP450 studies, rhCYP2D6*1/*1 or rhCYP2D6*10/*10 (8 pmol/ml) were preincubated with 2 μM VEN, ZJP (0.71–287.56 μg/ml for CYP2D6*1/*1 and 0.142–575.12 μg/ml for CYP2D6*10/*10), or its major components coptisine (0.1–100 μM for both CYP2D6s) and berberine (0.1–100 μM for CYP2D6*1/*1 and 0.05–100 μM for CYP2D6*10/*10) at 37°C for 5 minutes. All reactions were initiated with 10 mM NADPH, lasted for 15 minutes at 37°C, and were terminated with 200 μl of ice-cold acetonitrile. All reactions were quenched and treated as described above, and the supernatant was collected for LC-MS/MS analysis. The product formation data including ODV, NDV, or NODV was used for calculating enzymatic parameters.

Evaluation of the Influences of ZJP on the Metabolism and Pharmacokinetics of VEN in Rats. Twelve Wistar rats (male, 180–220 g) were randomly allocated into two groups ($n = 6$ in each group), which were blank control group and ZJP group. Twelve hours before the experiment, all rats were forbidden from eating except free access to water. Then each rat was intragastrically administered normal saline or ZJP solution (2.52 g/kg, dissolved in saline) at a single dose. Two hours after administration, rats were sacrificed, and liver samples were collected immediately on dry ice. All samples were stored at −80°C for further LC-MS/MS analysis.

Another 16 Wistar rats (male, 180–220 g) were also randomly divided into two groups ($n = 8$ in each group), which were blank control group and ZJP group. Each rat was intragastrically administered normal saline or ZJP solution (2.52 g/kg, dissolved in saline) once daily for 9 consecutive days. On the 9th day of administration, after 12 hours of fasting but free access to water, the rats in ZJP group received VEN (2.63 mg/kg) as well as ZJP, whereas the rats in blank control group received the same volume of normal saline. Blood samples were collected in heparinized tubes at 0, 0.5, 1, 1.5, 2, 3, 4, 6, 8, 12, 24, 36, and 48 hours after VEN administration and then centrifuged at 4000*g* 4°C for 10 minutes, and the plasma was collected and stored at −80°C for LC-MS/MS analysis.

Determination of Major Bioactive Components of ZJP in Rat Livers. Four major alkaloids (berberine, coptisine, evodiamine, and rutaecarpine) of ZJP in rat livers were quantitatively determined by a validated LC-MS/MS method. The LC-MS/MS system contained an LC20AD liquid chromatography (Shimadzu, Kyoto, Japan) and an API 4000 QTRAP triple quadrupole mass spectrometer (Applied Biosystems, Foster City, CA) equipped with an electrospray ionization source. Chromatographic separation was performed on an Agilent Eclipse XDB C_{18} reversed-phase column (150 × 4.6 mm, 5 μm) at room temperature. The gradient of the mobile phase consisting of water (0.08% formic acid and 4 mM ammonium acetate) (A) and acetonitrile (B) with a flow rate of 0.8 ml/min was set as follows: 0–3 minutes, 65% A; 3–4.5 minutes, 65%–20% A; 4.5–9 minutes, 20% A; 9–11 minutes, 20%–65% A; and 11–15 minutes, 65% A. Positive ionization mode and multiple reaction monitoring mode were selected for quantification. The parameters of mass spectrometry for each analyte were shown in Supplemental Table 2. The intra- and interday precision and accuracy of the quality control samples for each analyte were <15% (Supplemental Table 3). All analytes were stable in the measurement circumstances (Supplemental Table 4).

Determination of VEN and Its Three Metabolites in In Vitro and In Vivo Samples. VEN and its three metabolites (ODV, NDV, and NODV) from in vitro samples, such as HLMs, RLMs, or rhCYP2D6 reaction samples, and in vivo samples, such as rat plasma and liver samples, were quantitatively determined by a validated LC-MS/MS method. The LC-MS/MS system contained an Agilent-1260 liquid chromatograph (Agilent Technologies, Santa Clara, CA) and an API 4000 triple quadrupole mass spectrometer (Applied Biosystems) equipped with an electrospray ionization source. Chromatographic separation was performed on a Phenomenex Kinetex XB-C18 reversed-phase column (100 × 4.6 mm, 5 μm) at 40°C. The gradient of the mobile phase consisting of water (0.1% formic acid and 5 mM ammonium acetate) (A) and methanol (B) with a flow rate of 1 ml/min was set as follows: 0–1 minutes, 60% A; 1–4 minutes, 60%–20% A; 4–5.5 minutes, 20% A; 5.5–5.6 minutes, 20%–60% A; and 5.6–8 minutes, 60% A. Positive ionization mode and multiple reaction monitoring mode were selected for quantification. The parameters of mass spectrometry for each analyte were shown in Table 1. Linear calibration curves for VEN, ODV, NDV, and NODV were constructed in relative matrices with concentrations ranging 2.5–2000, 0.35–280,

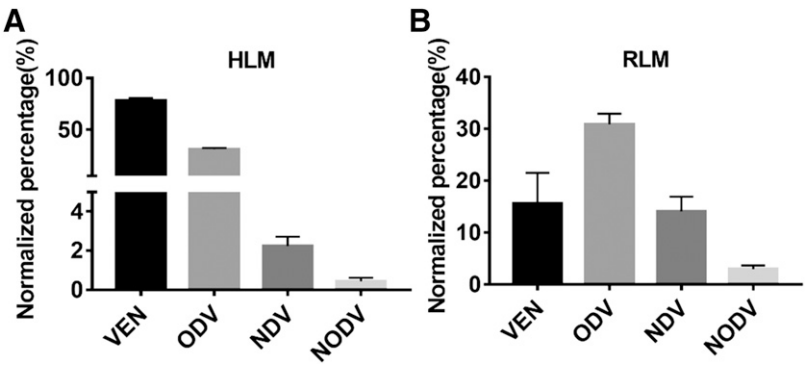

Fig. 2. The remaining VEN and generated demethylation metabolites, ODV, NDV, and NODV, after 60-minute incubation of VEN in HLM (A) or RLM (B). Data for each component were normalized to spiked VEN concentration in reaction mixtures and represented as means ± S.D. in triplicates.

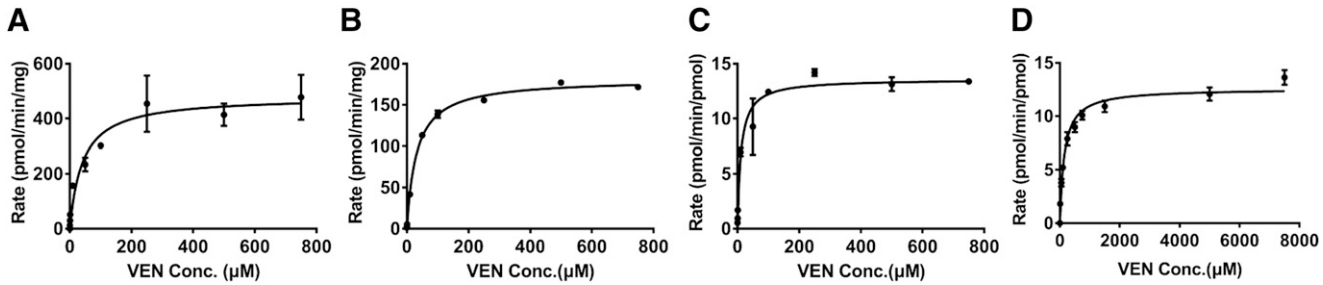

Fig. 3. Michaelis-Menten plots for formation of ODV by RLM (A), HLM (B), CYP2D6*1/*1 (C), and CYP2D6*10/*10 (D). Data were presented as means ± S.D. in triplicates.

0.35–280, and 0.7–560 nM, respectively. The intra- and interday precision and accuracy of the quality control samples for each analyte were <15% (Supplemental Table 5).

Data Analysis. The elimination half-life of VEN was estimated as the following:

$$k = -\ln([S]_t/[S]_0)/t \quad (1)$$

$$T_{1/2} = 0.693/k \quad (2)$$

where t referred to the incubation time, S represented the remaining parent drug concentration, and k indicated the first-order rate constant (Obach et al., 1997).

The intrinsic clearance (CL_{int}) of VEN determined in HLM and RLM was directly obtained from k as the following:

$$CL_{int} = k \times ml \cdot incubation/mg \cdot micorosomes. \quad (3)$$

Apparent kinetic parameters [e.g., V (reaction velocity), K_m (Michaelis-Menten constant), and V_{max} (maximum reaction velocity)] of the *O*-demethylation metabolism of VEN were obtained by fitting the substrate concentrations and initial reaction rates by using Michaelis-Menten equation as the following:

$$V = V_{max}[S]/(K_m + [S]) \quad (4)$$

$$CL_{int} = V_{max}/K_m \quad (5)$$

where S referred to substrate, and V, V_{max}, and K_m were the same as above.

IC_{50} (concentration with 50% inhibition) was calculated as the following:

$$Y = Bottom + (Top\text{-}Bottom)/(1 + 10\text{^}((LogIC_{50}\text{-}X)HillSlope))$$

where X referred to log (inhibitor concentration), Y referred to percent inhibition, Top and Bottom referred to maximum and minimum value of Y, and Hill Slope referred to curve slope.

Statistics. The data were expressed as means ± S.D. One-way ANOVA after the least significant difference method was used for the comparisons between control and test groups. A two-sided *P* value <0.05 was considered statistically significant. Data analysis and graphs were generated using GraphPad Prism software (version 7.0; Graphpad Software Inc., La Jolla, CA).

Results

Metabolic Stability of VEN in HLM and RLM. After a 60-minute incubation, the remaining VEN in RLM and HLM were 15.6% and 78.3%, respectively, indicating a faster phase I metabolism of VEN in rats than in humans (Fig. 2). In both RLM and HLM, ODV was the primary metabolite (30.9% vs. 31.0%), whereas NDV was 6.3-fold higher in RLM than HLM (14.1% vs. 2.2%), indicating a species difference in the metabolism of VEN.

Enzymatic Kinetics of VEN in HLM, RLM, and rhP450s. Because ODV was the dominant metabolite of VEN, we explored its generating rate to reflect the enzymatic kinetics of VEN in RLM, HLM, and rhP450s, respectively (Fig. 3; Table 2). In the RLM and HLM experiments, although K_m was very similar, the V_{max} of RLM was 6.6-fold higher than that of HLM. Hence, there was a 2.1-fold increase comparing CL_{int} of VEN in RLM to that in HLM (Fig. 3, A and B). In the rhP450 experiments, the two rhCYP2D6s with different alleles, *1/*1 and *10/*10, showed similar V_{max} values (0.014 vs. 0.013 nmol/min per picomoles P450), whereas the CYP2D6*10/*10 showed a 13.1-fold higher K_m value than that of CYP2D6 *1/*1, resulting in a 14.0-fold lower CL_{int} than CYP2D6*1/*1 (Fig. 3, C and D).

Influence of ZJP and Its Major Components on the Metabolism of VEN in HLM and RLM. To explore whether ZJP could influence the demethylation process of VEN, ZJP and its main components, berberine and coptisine, were incubated with VEN (1 μM) in HLM and RLM, respectively (Fig. 4). The results showed that ZJP significantly inhibited VEN depletion (94.5%) and the formation of its demethylation products, ODV, NDV, and NODV (91.0%, 69.4%, and 66.5%, respectively), compared with the control group in HLM (all *P* values <0.001) (Fig. 4, A–D). Coptisine and berberine demonstrated a similar tendency as ZJP. CYP2D6 was primarily responsible for the metabolism of VEN and the generation of ODV in HLM, which were inhibited by QND at inhibitory degrees of 96.5% and 95.6%, respectively. Meanwhile, NDV increased by 33.7% compared with the control group after QND treatment. In contrast, KTZ significantly inhibited the production of NDV and NODV (both $P < 0.001$) but without obvious effect on ODV ($P = 0.557$).

Similarly, the VEN depletion and formation of ODV and NODV significantly decreased after ZJP (48.3%, 33.0%, and 78.9%, respectively) and coptisine (19.8%, 13.5%, and 53.8%, respectively) treatment in RLM (all *P* values <0.05) (Fig. 4, E–H). Meanwhile, NDV increased by 73.5%, 66.8%, and 86.3% in the presence of ZJP, coptisine, and berberine, respectively. Interestingly, ZJP exhibited very similar tendencies in either VEN depletion or its metabolite generation as that of QNN, a specific inhibitor of rat CYP2D, and KTZ, indicating that CYP3A4 could also play an important role in the metabolism of VEN in rats.

IC_{50} of ZJP and Its Major Components on the Metabolism of VEN in HLM, RLM, and rhCYP2D6s. To further disclose the inhibitory potency of ZJP and its major bioactive components on the metabolism of VEN, the inhibitory effects, or IC_{50}, of ZJP, coptisine, or berberine on ODV production in microsomes or on rhCYP2D6s were investigated subsequently (Fig. 5). The individual IC_{50} values of ZJP, berberine, and coptisine on the metabolism of VEN are shown in

TABLE 2

Enzymatic kinetics parameters of VEN in RLM, HLM, and rhCYP2D6s

Subject	K_m (μM)	V_{max} (nmol/min per Milligram Protein or nmol/min per Picomoles P450)	CL_{int} (μl/min per Milligram Protein or μl/min per Picomoles P450)
RLM	41.2 ± 23.4	0.480 ± 0.013	11.7 ± 5.5
HLM	39.9 ± 1.1	0.182 ± 0.004	5.7 ± 0.2
rhCYP2D6*1/*1	11.3 ± 3.2	0.014 ± 0.003	1.2 ± 0.3
rhCYP2D6*10/*10	148.2 ± 26.5	0.013 ± 0.002	0.088 ± 0.016

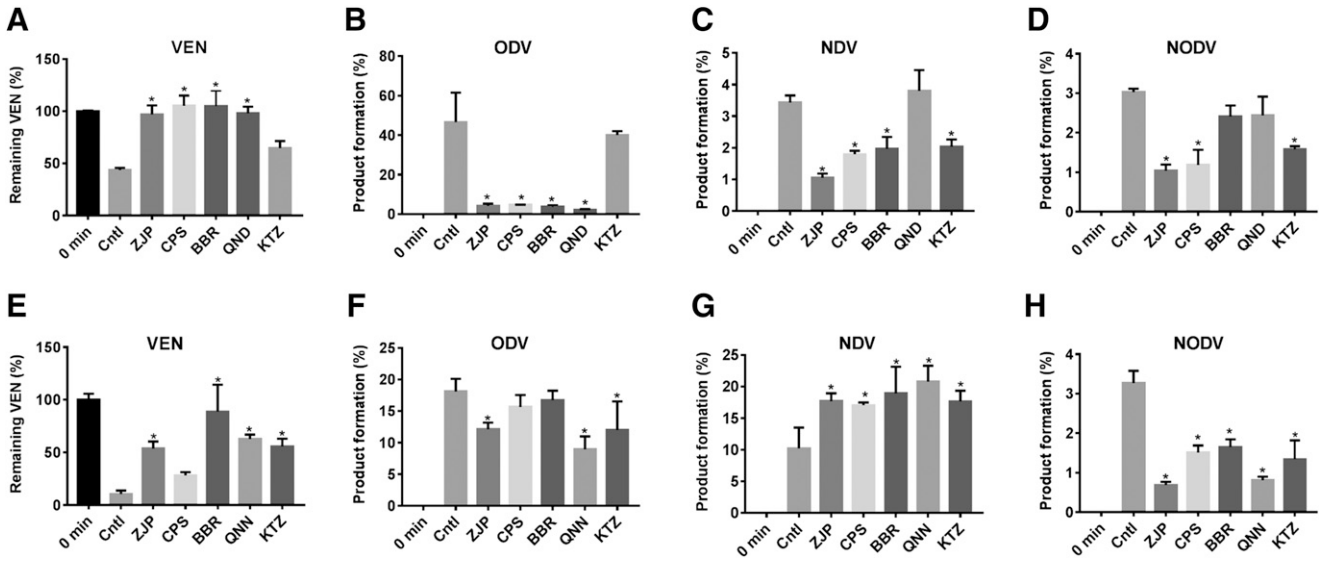

Fig. 4. Inhibitory effects of ZJP (150 μg/ml), coptisine (CPS, 30 μM), berberine (BBR, 30 μM), quinine (QNN, 2 μM), quinidine (QND, 2 μM), and ketoconazole (KTZ, 2 μM) on the metabolism of VEN and formation of ODV, NDV, and NODV in HLM (A–D) and RLM (E–H). Each column represented the remaining VEN (% control) or product formation (% spiked VEN). Data were presented as means ± S.D. in triplicates. *$P < 0.05$ compared with the control. Cntl, control.

Table 3. Those results showed that ZJP, coptisine, and berberine could inhibit the *O*-demethylation of VEN while showing little effect (IC_{50} > 280 μg/ml or 100 μM) on the *N*-demethylation process of VEN. In addition, ZJP and its two bioactive components exhibited higher inhibitory potency in HLM compared with RLM. Meanwhile, coptisine was more potent than berberine in inhibiting the formation of ODV and NODV, as it displayed lower IC_{50} values both in HLM and RLM (7.5% and 41.9%, respectively) than those of berberine. Both coptisine and berberine were potent inhibitors of rhCYP2D6*1/*1 and rhCYP2D6*10/*10, as IC_{50} values did not exceed 2.5 μM. As NDV and NODV were not

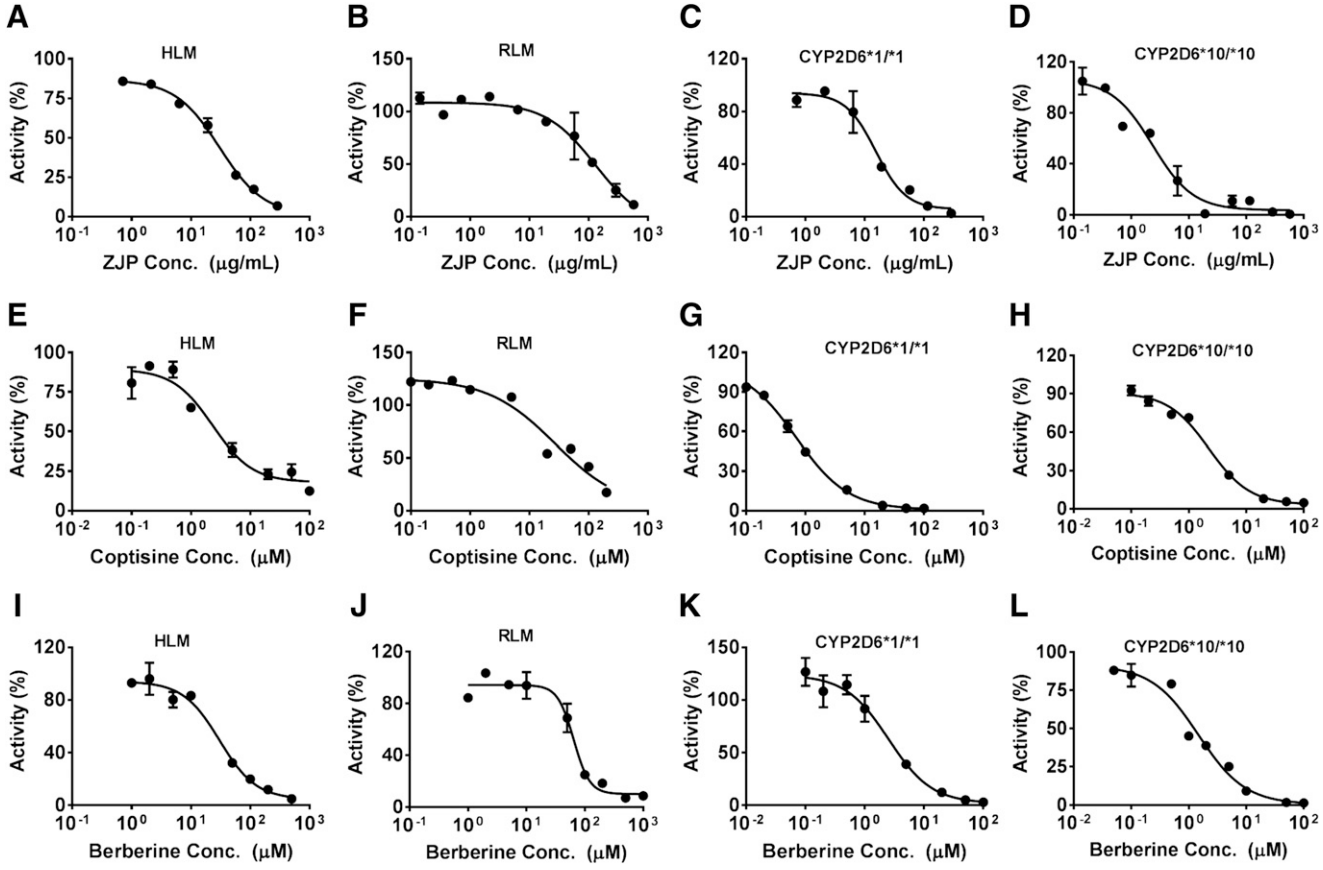

Fig. 5. Inhibitory effects (IC_{50}) of ZJP (A–D), coptisine (E–H), and berberine (I–L) on ODV formation in HLM, RLM, CYP2D6*1/*1, and CYP2D6*10/*10, respectively. Data were presented as means ± S.D. in triplicates. The curve represented the fitting of the observed ODV formation rate (% control) (*y*) vs. the inhibitor concentration (*x*). Conc., concentration.

TABLE 3

IC_{50} of ZJP, berberine, and coptisine toward VEN metabolism in microsomes and rhCYP2D6

	Inhibitors	IC_{50} value ODV	NDV	NODV
RLM	ZJP (μg/ml)	129.9 ± 2.6	>575	42.8 ± 8.0
	Berberine (μM)	64.5 ± 11.5	>1000	59.5 ± 18.6
	Coptisine (μM)	27.0 ± 6.2	>200	16.9 ± 0.1
HLM	ZJP (μg/ml)	30.5 ± 5.5	>288	11.5 ± 10.2
	Berberine (μM)	30.5 ± 9.6	>500	>500
	Coptisine (μM)	2.3 ± 1.3	>100	>100
rhCYP2D6*1/*1	ZJP (μg/ml)	15.4 ± 4.5	N/A	N/A
	Berberine (μM)	2.5 ± 0.9		
	Coptisine (μM)	0.7 ± 0.2		
rhCYP2D6*10/*10	ZJP (μg/ml)	2.3 ± 1.0	N/A	N/A
	Berberine (μM)	1.5 ± 0.2		
	Coptisine (μM)	2.2 ± 0.2		

N/A, not applicable.

detected in rhCYP2D6s but in microsomes, other P450s than CYP2D6 were responsible for the *N*-demethylation process of VEN.

Inhibitory Effects of ZJP on the Metabolism of VEN and Pharmacokinetics in Rats. VEN and its major metabolites, ODV and NDV, were detected in rat plasma after intragastric administration of VEN alone or coadministration with ZJP (VEN+ZJP). The mean plasma concentration-time curves are plotted in Fig. 6. The pharmacokinetic parameters of VEN and its metabolites were presented in Table 4. Compared with the VEN group, the AUC_{0-24} for VEN and ODV increased obviously by 39.6% and 22.8%, respectively, in the VEN+ZJP group; meanwhile, AUC_{0-24} of NDV increased dramatically ($P < 0.05$) in the VEN+ZJP group.

VEN and its metabolites ODV, NDV, and NODV, were detected in the liver 2 hours after intragastric administration of VEN alone or coadministration with ZJP (VEN+ZJP) (Fig. 7). Compared with the VEN group, after coadministration with ZJP, the ODV exposure in the liver decreased significantly by 57.2% (P = 0.014), whereas NDV exposure increased significantly by 72.7% in VEN+ZJP group (P = 0.014). Meanwhile, the ratio of ODV/VEN in the liver also decreased significantly by 37.7% (P = 0.018) upon ZJP administration.

Discussion

Depression is the leading cause of psychiatric disorders, with an estimated 350 million people affected worldwide (Cipriani et al., 2018). Depression can be long-lasting or recurrent, and it can dramatically affect people's ability to live a rewarding life. VEN, approved in 1995, is a classic antidepressant, but it still stands as one of the most efficacious and prescribed antidepressants, particularly for the treatment of selective serotonin reuptake inhibitor-resistant depression (Cipriani et al., 2018). VEN undergoes extensive phase I metabolism and is primarily catalyzed by CYP2D6 to generate an active metabolite, ODV. The recommended therapeutic reference range for VEN is 100–400 ng/ml of active moiety, which is calculated from the total amount of VEN and ODV (Hiemke et al., 2018). The metabolic ratio ODV/VEN is usually used as a tool to distinguish patients as poor metabolizers or extensive metabolizers of CYP2D6 (Lobello et al., 2010). When VEN is coadministered with a CYP2D6 inhibitor such as paroxetine, both C_{max} and AUC of VEN are significantly elevated in patients, which might explain VEN responses and adverse events (Jiang et al., 2015). Although the discrepancy on the clinical implication of exposure changes to VEN and/or ODV is still great, knowledge of the mechanisms of potential DDI between VEN and a drug with CYP2D6 inhibition is necessary for assessing and minimizing clinical risks (Schoretsanitis et al., 2019).

Traditional Chinese medicines (TCMs) belong to herbal medicines and have a long history of usage in clinical practice. In Asia, TCMs are prescribed concomitantly with conventional medications (prescription and nonprescription) for treatments. However, the risk assessment of the pharmacokinetic interaction between TCMs and conventional drugs is insufficient, leading to safety and efficacy issues in contemporary pharmacotherapy. ZJP is a widely used traditional Chinese herbal formula recorded in the Chinese Pharmacopoeia for routine treatments of gastrointestinal disorders (Chinese Pharmacopoeia Commission, 2015). It is commonly prescribed to patients with indications of gastritis, such as gastric ulcer, pyloric obstruction, gastroesophageal reflux disease, etc. It is also beneficial for depression with maladjusted gastrointestinal function (Wang et al., 2020). ZJP consists of two commonly used herbs, *Rhizoma Coptidis* and *Fructus Evodiae*, following a 6:1 (w/w) ratio. *Rhizoma Coptidis* is reported to inhibit

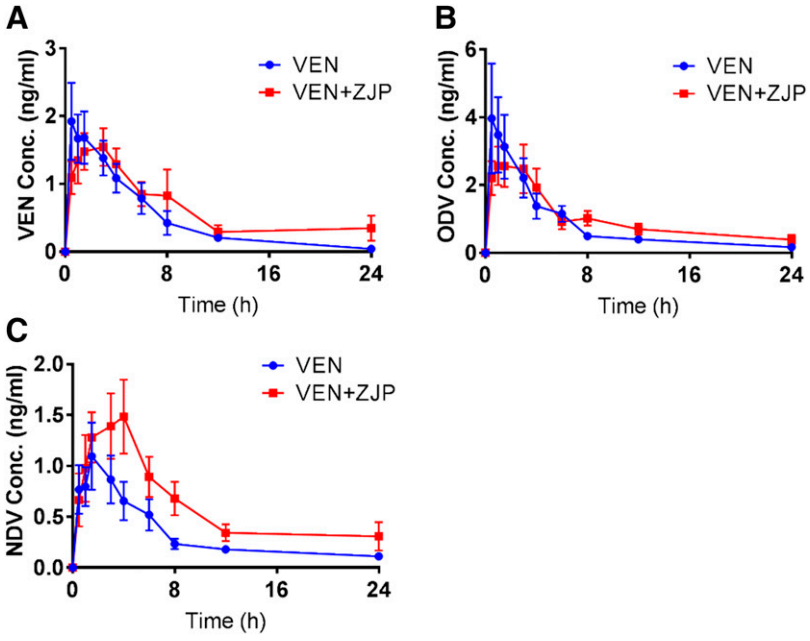

Fig. 6. Mean plasma concentration-time profiles of VEN (A), ODV (B), and NDV (C) after intragastric administration of VEN alone or coadministration with ZJP (VEN+ZJP) in rats (n = 6). Data were presented as means ± S.D. Conc., concentration.

TABLE 4

Pharmacokinetic parameters of VEN, ODV, and NDV in rats after oral administration of VEN alone or VEN combined with ZJP

Analyte	Groups	C_{max} (ng/ml)	T_{max} (h)	$t_{1/2}$ (h)	CLz/F (l/h per kilogram)	AUC_{0-24} (μg/l × h)
VEN	VEN	3.47 ± 0.80	1.0 ± 0.6	2.4 ± 2.2	231.7 ± 18.6	11.1 ± 0.9
	VEN+ZJP	2.01 ± 0.85*	3.1 ± 1.8*	4.0 ± 2.2	198.7 ± 151.3	15.5 ± 7.6
ODV	VEN	4.82 ± 4.18	1.1 ± 0.9	6.2 ± 3.3	172.7 ± 123.5	19.3 ± 11.3
	VEN+ZJP	3.41 ± 2.00	2.1 ± 1.4	10.9 ± 6.5	116.8 ± 66.8	23.7 ± 12.8
NDV	VEN	1.24 ± 0.90	2.0 ± 1.8	5.1 ± 2.9	468.0 ± 208.7	6.45 ± 4.34
	VEN+ZJP	1.91 ± 1.02	3.6 ± 2.2	6.1 ± 4.5	215.4 ± 132.1*	13.5 ± 5.7*

*$P < 0.05$ compared with VEN group. CLz/F, apparent oral clearance.

CYP2D6 activity with an IC_{50} value of 5.8 μg/ml of its extracted powder (approximately equal to 30.4 μg/ml of crude herbs) in HLM (Han et al., 2011). The inhibitory effect might be mostly attributable to Coptis alkaloid components, especially coptisine, with an IC_{50} value of 4.4 μM (Han et al., 2011). Moreover, when ZJP is coadministered with dextromethorphan, a known CYP2D6 substrate, the $AUC_{0-24\ hour}$ of dextromethorphan in healthy volunteers with dominant CYP2D6 phenotype (CYP2D6*1/*1) increases 3.0-fold higher than those administered dextromethorphan only (Qiu et al., 2016). With the high likelihood of combination usage of the two conventional prescriptions ZJP and VEN for treating depression patients with gastrointestinal disorders in China and potential herb-drug interaction (Qiu et al., 2015; Wang et al., 2020), we investigated the pharmacokinetic influences of ZJP on VEN for the first time. In this study, we found that ZJP significantly inhibits the metabolism of VEN in vitro. After coincubation of VEN and ZJP for 1 hour, the VEN depletion and ODV formation decreased significantly by 94.5% and 91.0%, respectively, compared with the blank control in HLM and, similarly, by 48.3% and 33.0% respectively, compared with the blank group in RLM. It was supported by IC_{50} values of ZJP determined by ODV formation with 30.5 and 129.9 μg/ml for HLM and RLM, respectively. Aside from the minor inhibitory effects of *Fructus Evodiae* on CYP2D6, the IC_{50} values of ZJP (approximately equal to 26.2 μg/ml of crude herbs of *Rhizoma Coptidis*) on VEN were similar to those reported on dextromethorphan (30.4 μg/ml of crude herbs of *Rhizoma Coptidis*) (Han et al., 2011). We also observed that ZJP inhibited the pharmacokinetics and tissue distribution of VEN in rats. ZJP increased AUC_{0-24} of VEN by 39.6% in rats, and 2 hours after coadministration of VEN with ZJP, the hepatic exposure of ODV was reduced by 57.2% ($P = 0.014$). Those findings suggested a potential human DDI between ZJP and VEN, although not firmly supported by some DDI data in rats. In addition, it was worth mentioning that because of focuses on the plasma exposure of VEN (between 100 and 400 ng/ml) in clinical practice that was far below the K_m values obtained both in HLM and RLM, we selected a clinically relevant VEN concentration, e.g., 0.5 or 1 μM, for IC_{50} experiments.

Species difference is probably the reason for weak evidence of DDI potential between ZJP and VEN in rats. CYP2D isoforms between rats and humans share a good homology (>70%) (Venhorst et al., 2003). Rat CYP2D1 is known as an ortholog (approximately 83% homology) of human CYP2D6 (Martignoni et al., 2006). However, when comparing the metabolic capability of VEN, the two species are obviously different. In literatures, the C_{max} and $AUC_{0-\infty}$ of VEN in poor metabolizerss increased by approximately 70%–80% and 200%–300%, respectively, compared with those of extensive metabolizers (Lessard et al., 1999; Lobello et al., 2010). In contrast, the C_{max} and $AUC_{0-\infty}$ of VEN in CYP2D1-null rats only increased by 24% and 59%, respectively, compared with those of wild-type rats, indicating an apparently weaker inhibitory effect involved in CYP2D6 inhibition in rats than humans (Zhou et al., 2019). Similarly, we observed that the capability and magnitude of inhibitory effects of ZJP were not comparable between HLM and RLM. First, the metabolic characteristics of VEN were different between the two species. CYP2D6 was the sole principle P450

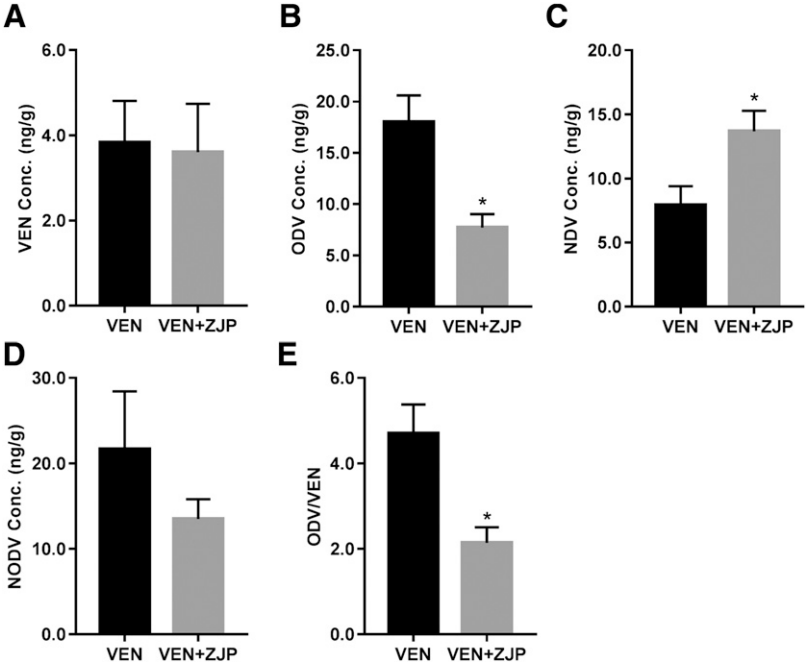

Fig. 7. Hepatic exposures of VEN (A), ODV (B), NDV (C), NODV (D), and ODV/VEN ratio (E) at 2 hours after intragastric administration of VEN alone or coadministration with ZJP (VEN+ZJP) in rats ($n = 6$). Data were presented as means ± S.D. *$P < 0.05$ compared with the VEN group. Conc., concentration.

enzyme responsible for VEN metabolism in HLM but not in RLM. After 1 hour of incubation of VEN, ODV (generated primarily by CYP2D6) was the major metabolite (31.0% of spiked VEN), and NDV (generated primarily by CYP3A4 and CYP2C19) was the minor metabolite (2.2% of spiked VEN) in HLM. In contrast, ODV and NDV were both major metabolites in RLM, with 30.9% and 14.1% of formation rate percentages, respectively. Secondly, the inhibitory effects of CYP2D6 inhibitor on ODV formation in rats were weaker than those in humans. Quinidine, a known human CYP2D6 inhibitor, inhibited VEN depletion (96.5%) and ODV formation (95.6%) completely in HLM. In contrast, quinine, the quinidine enantiomer and a known rat CYP2D6 inhibitor, inhibited VEN depletion (58.4%) and ODV formation (50.6%) partly in RLM. The inhibitory efficacy (IC_{50} values obtained from ODV formation) of the potent CYP2D6 inhibitor in HLM was greater than that in RLM (10.0 μM vs. 31.5 μM) (Supplemental Fig. 1). Taken together, CYP2D6 (in fact CYP2D1 in rats) did not play a dominant role in VEN metabolism in RLM as it did in HLM, and there were possibly other P450s involved in ODV formation in RLM. In the study, we observed that ketoconazole, a known CYP3A4 inhibiter, could also significantly inhibit ODV formation in RLM, but it showed negligible inhibition in HLM. Therefore, the underestimated risks of predicting the magnitude of DDI between ZJP and VEN in humans through rat DDI data based only on the enzymatic activity of CYP2D6 should be seriously noted. Considering that ZJP could increase the $AUC_{0-24\ hour}$ of dextromethorphan, a sensitive index substrate of CYP2D6, in healthy CYP2D6*1/*1 carriers by 3.0-fold greater, further studies were merited to explore ZJP and VEN interaction in humans (Qiu et al., 2016).

Similar to previous research, we had determined extremely low systemic exposures for the four major alkaloid constituents, berberine, coptisine, evodiamine, and rutaecarpine, in rats after intragastric administration of ZJP. Only berberine could be detected in some time intervals, and the average of C_{max} was below 50 ng/ml; however, the other three alkaloids, coptisine, evodiamine, and rutaecarpine, were detected below the limit of detection of 1.0 ng/ml during the whole blood sampling period (data not shown). The observation showed strong consistency with previous research, in that those alkaloids possessed the characteristics of low bioavailability, either in animals or humans (Yan et al., 2011; Qian et al., 2017; Wang et al., 2018; Zhang et al., 2018). For example, after single oral administration of *Rhizoma Coptidis* granules in healthy volunteers (which contain 20 mg/kg of berberine and are approximately 1.8-fold higher than rat dosage in the animal experiment when converted equivalently based on body surface area), the average plasma C_{max} of berberine is still as low as 360.9 ± 46.1 ng/ml (Huang et al., 2011). Thus, an interesting question will be raised as to why there is increasing evidence that many herbs containing active alkaloids with low bioavailability have pharmacokinetic interactions with other coadministered drugs. The underlying mechanism may be multiple principles involving one or more processes of absorption, disposition, metabolism, and excretion. In this study, we found that the concentrations of Coptis alkaloids berberine and coptisine in liver tissue were much higher (>10.0-fold higher) than those in plasma, which was in accordance with previous literature (Liu et al., 2010). Although the concentration of single alkaloids in the rat liver (e.g., 25.5 and 3.1 mg/g for berberine and coptisine, respectively) for CYP2D6-mediated metabolism of VEN was slightly lower than the IC_{50} (e.g., 21.7 and 8.6 mg/g for berberine and coptisine, respectively), considering the structural and mechanistic similarities of the alkaloids in ZJP, whether determined, the synergistic effects should be considered seriously. Furthermore, several Coptis alkaloids (such as berberine) might have cumulative effects with multiple dosing (Ma and Ma, 2013). This might be one of the main reasons for the herb-drug interaction induced by the herbs containing Coptis alkaloids.

In conclusion, Zuojin Pill has significant inhibitory effects on hepatic metabolism and pharmacokinetics of venlafaxine in vitro and in rats, mainly through suppression of CYP2D6 activity. In view of the species differences in the role of CYP2D6 involved with venlafaxine metabolism, the human pharmacokinetic interaction between Zuojin Pill and venlafaxine and its related clinical significance need to be seriously considered.

Authorship Contributions

Participated in research design: Tan, Qiu.
Conducted experiments: Y. Li, J. Li, Yan, Wang, Jin, Tan.
Performed data analysis: Y. Li, Tan, Qiu.
Wrote or contributed to the writing of the manuscript: Y. Li, Tan, Qiu.

References

Chinese Pharmacopoeia Commission (2015) Zuojin Wan, *The Pharmacopoeia of the People's Republic of China* pp 763–764, China Medical Science Press, Beijing, China.

Cipriani A, Furukawa TA, Salanti G, Chaimani A, Atkinson LZ, Ogawa Y, Leucht S, Ruhe HG, Turner EH, Higgins JPT, et al. (2018) Comparative efficacy and acceptability of 21 antidepressant drugs for the acute treatment of adults with major depressive disorder: a systematic review and network meta-analysis. *Lancet* **391**:1357–1366.

Fogelman SM, Schmider J, Venkatakrishnan K, von Moltke LL, Harmatz JS, Shader RI, and Greenblatt DJ (1999) O- and N-demethylation of venlafaxine in vitro by human liver microsomes and by microsomes from cDNA-transfected cells: effect of metabolic inhibitors and SSRI antidepressants. *Neuropsychopharmacology* **20**:480–490.

Gao X, Yang XW, and Marriott PJ (2010) Simultaneous analysis of seven alkaloids in Coptis-Evodia herb couple and Zuojin pill by UPLC with accelerated solvent extraction. *J Sep Sci* **33**: 2714–2722.

Han YL, Yu HL, Li D, Meng XL, Zhou ZY, Yu Q, Zhang XY, Wang FJ, and Guo C (2011) In vitro inhibition of Huanglian [Rhizoma coptidis (L.)] and its six active alkaloids on six cytochrome P450 isoforms in human liver microsomes. *Phytother Res* **25**:1660–1665.

Hiemke C, Bergemann N, Clement HW, Conca A, Deckert J, Domschke K, Eckermann G, Egberts K, Gerlach M, Greiner C, et al. (2018) Consensus guidelines for therapeutic drug monitoring in neuropsychopharmacology: update 2017. *Pharmacopsychiatry* **51**:e1.

Huang Z, Lu F, Dong H, Xu L, Chen G, Zou X, and Lei H (2011) Effects of cinnamon granules on pharmacokinetics of berberine in Rhizoma Coptidis granules in healthy male volunteers. *J Huazhong Univ Sci Technolog Med Sci* **31**:379–383.

Jiang F, Kim HD, Na HS, Lee SY, Seo DW, Choi JY, Ha JH, Shin HJ, Kim YH, and Chung MW (2015) The influences of CYP2D6 genotypes and drug interactions on the pharmacokinetics of venlafaxine: exploring predictive biomarkers for treatment outcomes. *Psychopharmacology (Berl)* **232**:1899–1909.

Johnson EJ, González-Peréz V, Tian DD, Lin YS, Unadkat JD, Rettie AE, Shen DD, McCune JS, and Paine MF (2018) Selection of priority natural products for evaluation as potential precipitants of natural product-drug interactions: a NaPDI center recommended approach. *Drug Metab Dispos* **46**:1046–1052.

Lessard E, Yessine MA, Hamelin BA, O'Hara G, LeBlanc J, and Turgeon J (1999) Influence of CYP2D6 activity on the disposition and cardiovascular toxicity of the antidepressant agent venlafaxine in humans. *Pharmacogenetics* **9**:435–443.

Liu S, Qiu F, He M, Miu P, Zeng J, and Jiang J (2014) Research of constituents metabolism and effect for CYP450 of Zuojin Pill. *Acta Chinese Medicine* **29**:1622–1625.

Liu YT, Hao HP, Xie HG, Lai L, Wang Q, Liu CX, and Wang GJ (2010) Extensive intestinal first-pass elimination and predominant hepatic distribution of berberine explain its low plasma levels in rats. *Drug Metab Dispos* **38**:1779–1784.

Lobello KW, Preskorn SH, Guico-Pabia CJ, Jiang Q, Paul J, Nichols AI, Patroneva A, and Ninan PT (2010) Cytochrome P450 2D6 phenotype predicts antidepressant efficacy of venlafaxine: a secondary analysis of 4 studies in major depressive disorder. *J Clin Psychiatry* **71**:1482–1487.

Ma BL and Ma YM (2013) Pharmacokinetic properties, potential herb-drug interactions and acute toxicity of oral Rhizoma coptidis alkaloids. *Expert Opin Drug Metab Toxicol* **9**:51–61.

Magalhães P, Alves G, LLerena A, and Falcão A (2015) Clinical drug-drug interactions: focus on venlafaxine. *Drug Metab Pers Ther* **30**:3–17.

Martignoni M, Groothuis GM, and de Kanter R (2006) Species differences between mouse, rat, dog, monkey and human CYP-mediated drug metabolism, inhibition and induction. *Expert Opin Drug Metab Toxicol* **2**:875–894.

Nicolussi S, Drewe J, Butterweck V, and Meyer Zu Schwabedissen HE (2020) Clinical relevance of St. John's wort drug interactions revisited. *Br J Pharmacol* **177**:1212–1226.

Obach RS, Baxter JG, Liston TE, Silber BM, Jones BC, MacIntyre F, Rance DJ, and Wastall P (1997) The prediction of human pharmacokinetic parameters from preclinical and in vitro metabolism data. *J Pharmacol Exp Ther* **283**:46–58.

Otton SV, Ball SE, Cheung SW, Inaba T, Rudolph RL, and Sellers EM (1996) Venlafaxine oxidation in vitro is catalysed by CYP2D6. *Br J Clin Pharmacol* **41**:149–156.

Paine MF and Oberlies NH (2007) Clinical relevance of the small intestine as an organ of drug elimination: drug-fruit juice interactions. *Expert Opin Drug Metab Toxicol* **3**:67–80.

Qian P, Zhang Y-B, Yang Y-F, Xu W, and Yang X-W (2017) Pharmacokinetics studies of 12 alkaloids in rat plasma after oral administration of Zuojin and Fan-Zuojin formulas. *Molecules* **22**:214.

Qiu C, Cui YL, Qi XJ, Jiang HL, and Wang QS (2015) [Advance in modern studies on compatibility of Coptidis Rhizoma and Evodiae fructus]. *Zhongguo Zhongyao Zazhi* **40**:582–587.

Qiu F, Liu S, Miao P, Zeng J, Zhu L, Zhao T, Ye Y, and Jiang J (2016) Effects of the Chinese herbal formula "Zuojin Pill" on the pharmacokinetics of dextromethorphan in healthy Chinese volunteers with CYP2D6*10 genotype. *Eur J Clin Pharmacol* **72**:689–695.

Schoretsanitis G, Haen E, Gründer G, Hiemke C, Endres K, Ridders F, Correll CU, and Paulzen M (2019) Pharmacokinetics of venlafaxine in treatment responders and non-responders: a retrospective analysis of a large naturalistic database. *Eur J Clin Pharmacol* **75**:1109–1116.

Venhorst J, ter Laak AM, Commandeur JN, Funae Y, Hiroi T, and Vermeulen NP (2003) Homology modeling of rat and human cytochrome P450 2D (CYP2D) isoforms and computational rationalization of experimental ligand-binding specificities. *J Med Chem* **46**:74–86.

Wang LY, Tang YP, Liu X, Ge YH, and Li WX (2013) [Research on Chinese medicine pairs (VI)--Coptidis Rhizoma-Euodiae fructus]. *Zhongguo Zhongyao Zazhi* **38**:4214–4219.

Wang T, Yan YF, Yang L, Huang YZ, Duan XH, Su KH, and Liu WL (2020) Effects of Zuojin pill on depressive behavior and gastrointestinal function in rats with chronic unpredictable mild stress: role of the brain-gut axis. *J Ethnopharmacol* **254**:112713.

Wang Y, Zhang Y, Xiao J, Xu R, Wang Q, and Wang X (2018) Simultaneous determination of baicalin, baicalein, wogonoside, wogonin, scutellarin, berberine, coptisine, ginsenoside Rb1 and ginsenoside Re of Banxia xiexin decoction in rat plasma by LC-MS/MS and its application to a pharmacokinetic study. *Biomed Chromatogr* **32**:e4083.

Yan R, Wang Y, Shen W, Liu Y, and Di X (2011) Comparative pharmacokinetics of dehydroevodiamine and coptisine in rat plasma after oral administration of single herbs and Zuojinwan prescription. *Fitoterapia* **82**:1152–1159.

Zhang QS, Wang GW, Han ZQ, Chen XM, Na R, Jin H, Li P, and Bu R (2018) Metabolic profile of Rhizoma coptidis in human plasma determined using ultra-high-performance liquid chromatography coupled with high-resolution mass spectrometry. *Rapid Commun Mass Spectrom* **32**:63–73.

Zhou H, Yang L, Wang C, Li Z, Ouyang Z, Shan M, Gu J, and Wei Y (2019) *CYP2D1* gene knockout reduces the metabolism and efficacy of venlafaxine in rats. *Drug Metab Dispos* **47**: 1425–1432.

Address correspondence to: Bo Tan, Laboratory of Clinical Pharmacokinetics, Shuguang Hospital Affiliated to Shanghai University of TCM, 528 Zhangheng Rd., Shanghai 201203, China. E-mail: tbot@163.com; or Furong Qiu, Laboratory of Clinical Pharmacokinetics, Shuguang Hospital Affiliated to Shanghai University of TCM, 528 Zhangheng Rd., Shanghai 201203, China. E-mail: furong_qiu@126.com